ORIGINAL ARTICLE

Effects of glucokinase haploinsufficiency on the pancreatic β-cell mass and function of long-term high-fat, high-sucrose diet-fed mice

Ikumi Shigesawa[1] (iD), Akinobu Nakamura[1]* (iD), Yuki Yamauchi[1] (iD), Shinichiro Kawata[1], Asuka Miyazaki[1], Hiroshi Nomoto[1], Hiraku Kameda[1] (iD), Yasuo Terauchi[2], Tatsuya Atsumi[1]

[1]Department of Rheumatology, Endocrinology and Nephrology, Faculty of Medicine and Graduate School of Medicine, Hokkaido University, Sapporo, Japan, and [2]Department of Endocrinology and Metabolism, Graduate School of Medicine, Yokohama City University, Yokohama, Japan

ABSTRACT

Aims/Introduction: We previously showed that glucokinase haploinsufficiency improves the glucose tolerance of *db/db* mice by preserving pancreatic β-cell mass and function. In the present study, we aimed to determine the effects of glucokinase haploinsufficiency on the β-cell mass and function of long-term high-fat, high-sucrose (HFHS) diet-fed mice.

Materials and Methods: Four-week-old male glucokinase haploinsufficient ($Gck^{+/-}$) mice and 4-week-old male wild-type ($Gck^{+/+}$) mice (controls) were each divided into two groups: an HFHS diet-fed group and a normal chow-fed group, and the four groups were followed until 16, 40 or 60 weeks-of-age. Their glucose tolerance, glucose-stimulated insulin secretion and β-cell mass were evaluated. In addition, islets were isolated from 40-week-old mice, and the expression of key genes was compared.

Results: $Gck^{+/-}$HFHS mice had smaller compensatory increases in β-cell mass and glucose-stimulated insulin secretion than $Gck^{+/+}$HFHS mice, and their glucose tolerance deteriorated from 16 to 40 weeks-of-age. However, their β-cell mass and glucose-stimulated insulin secretion did not decrease between 40 and 60 weeks-of-age, but rather, tended to increase, and there was no progressive deterioration in glucose tolerance. The expression of *Aldh1a3* in pancreatic islets, which is high in several models of diabetes and is associated with an impairment in β-cell function, was high in $Gck^{+/+}$HFHS mice, but not in $Gck^{+/-}$HFHS mice.

Conclusions: Glucokinase haploinsufficiency prevents the progressive deterioration of pancreatic β-cell mass/function and glucose tolerance in long-term HFHS diet-fed mice.

INTRODUCTION

More than 500 million people around the world are currently living with diabetes, the majority of whom have type 2 diabetes[1]. Because diabetes remains a substantial public health issue, there is an urgent need to further elucidate the pathogenesis of type 2 diabetes and to identify effective treatments for the disease. Although the pathophysiology of type 2 diabetes is complex and not yet fully understood, the progressive loss of β-cell mass and function are central to its pathophysiology[2–6].

Findings obtained through studies on many animal and human genetic models have shown that the activation of glucokinase improves pancreatic β-cell function and increases the mass[7–10]. Glucokinase is an enzyme responsible for the conversion of glucose to glucose 6-phosphate, and is expressed in the pancreatic endocrine cells, liver, brain and gastrointestinal tract[11,12]. In particular, glucokinase in the pancreatic endocrine cells and liver cells plays an important role in the regulation of systemic glucose metabolism. Since 2003, a number of glucokinase activators have been developed, some of which have been shown to be effective and safe in phase III clinical trials[13–18]. In addition, glucokinase activators have been shown to enhance

the function and proliferation of β-cells in clinical trials and in our studies of mice[19–21]. However, it has been reported that the efficacy of glucokinase activators is not maintained over the long term[22–26], suggesting that chronic glucokinase activation may in fact cause pancreatic β-cell failure[27,28].

Based on the above, we hypothesized that in the presence of conditions, such as type 2 diabetes, in which people are exposed to chronic hyperglycemia, the inactivation of glucokinase may preserve pancreatic β-cell over the long term[29]. To test this hypothesis, we previously investigated the effects of glucokinase haploinsufficiency on the glucose tolerance and β-cell mass/function of db/db mice, a genetically engineered model of obesity and diabetes[30]. The glucokinase-haploinsufficient db/db mice showed less glucose intolerance and had superior β-cell mass and insulin secretion than the db/db mice. Furthermore, deoxyribonucleic acid (DNA) microarray, real-time quantitative polymerase chain reaction (PCR), immunohistochemical and metabolomic analyses have shown that glucokinase haploinsufficiency in the islets of db/db mice reduces the expression of stress-related genes, increases the expression of transcription factors involved in β-cell function, such as MafA and Nkx6.1, reduces mitochondrial damage and improves intracellular metabolic patterns. However, the protective effect of glucokinase inhibition on β-cells has not been studied in a model of obesity and diabetes induced by an environmental factor, such as diet, which would be more consistent with the pathogenesis of type 2 diabetes in humans. Therefore, in the present study, we characterized the effects of glucokinase haploinsufficiency on the β-cell mass and function of long-term high-fat, high-sucrose (HFHS) diet-fed mice.

MATERIALS AND METHODS

Study design
Four-week-old male glucokinase-haploinsufficient (Gck^{+/−}) mice and 4-week-old male wild-type (Gck^{+/+}) mice (controls) were each divided into two groups: an HFHS diet-fed group and a normal chow (NC)-fed group, and these total four groups were followed until 16, 40 or 60 weeks-of-age. We measured the bodyweights and fed blood glucose concentrations of mice in each group over these periods, then carried out oral glucose tolerance testing (OGTT), followed by tissue collection, at 16, 40 or 60 weeks of age. Both glucose tolerance and glucose-stimulated insulin secretion (GSIS) were assessed by OGTT, and pancreatic β-cell mass was evaluated using pancreatic tissue sections. Subsequently, to identify differences in islet gene expression, we collected islets from 40-week-old Gck^{+/+}NC, Gck^{+/+}HFHS, Gck^{+/−}NC and Gck^{+/−}HFHS mice, and studied their gene expression using DNA microarray analysis (Gck^{+/+}HFHS vs Gck^{+/−}HFHS) and real-time quantitative PCR.

Animals
Gck^{+/+} mice and Gck^{+/−} mice were generated as previously described[31]. The mutant Gck allele in these mice affects the

expression of glucokinase in neuroendocrine cells, but not in hepatocytes[31]. In fact, the messenger ribonucleic acid (mRNA) expression of Gck in isolated islets from Gck^{+/−} mice was only approximately 50% of that in the Gck^{+/+} mice (Figure S1). The mice were maintained at 25°C, under a 12-h light/dark cycle, and had free access to drinking water and food.

Diet protocol
NC (MF; Oriental Yeast Co. Ltd., Tokyo, Japan) and the HFHS diet (58R3; TestDiet, Richmond, VA, USA) were used. Table S1 shows the energy composition of the diets.

Measurement of blood glucose concentration
Blood glucose concentration was measured using a Glutestmint (Sanwa Chemical, Nagoya, Japan).

Oral glucose tolerance testing
The OGTT was performed after 16 h of fasting. 1.5 mg of glucose per gram of bodyweight was administered orally, and blood samples were collected before, and 15, 30, 60 and 120 min after glucose loading. GSIS was assessed by plasma insulin concentration before and 15 min after glucose loading in the OGTT. Insulin concentration was determined with a Morinaga Ultra-sensitive Mouse/Rat Insulin ELISA Kit (Moringa Institute of Biological Science, Yokohama, Japan).

Assessment of β-cell mass with immunohistochemistry
Isolated pancreatic tissue was fixed in 4% paraformaldehyde at 4°C overnight. After paraffin embedding, 5-μm sections were cut and mounted on glass slides. To inactivate endogenous peroxidase activity, the sections were immersed in phosphate-buffered saline containing 3% (vol/vol) hydrogen peroxide and then in BLOXALL (Vector laboratories, Newark, NJ, USA) for 15 min each. The sections were then immunostained with goat anti-rabbit insulin antibody (diluted 1:1,000; Proteintech, Rosemont, IL, USA) and counterstained with hematoxylin. Pancreatic area and β-cell area were calculated using a BZ-II analyzer (Keyence Corporation, Osaka, Japan), and β-cell mass was assessed as follows: β-cell mass (mg) = β-cell area / pancreatic area × pancreatic weight (mg).

Islet isolation
Hanks' balanced salt solution (HBSS; Sigma-Aldrich, St. Louis, MO, USA) containing 0.9 mg/mL of collagenase from Clostridium histolyticum (Sigma-Aldrich) was prepared (collagenase-supplemented HBSS). The liver and intestine of each mouse were exposed, the ampulla of Vater was clamped to block bile drainage into the duodenum, and 2.5 mL of collagenase-supplemented HBSS was injected from the common bile duct toward the pancreatic duct. The distended pancreas was then removed and placed in a 50-mL tube containing 7.5 mL of collagenase-supplemented HBSS and incubated at 37°C for 24 min to digest the pancreas. After the digested pancreas had been dispersed by pipetting, it was washed with

HBSS containing fetal bovine serum to stop the digestive process. The resulting solution, containing separated islets, was transferred to a Petri dish, and the islets were collected using a pipette under a microscope.

DNA microarray analysis

RNA was extracted from isolated islets using an miRNeasy Micro Kit (Qiagen, Hilden, Germany). The mRNA expression profile of each was characterized using a Mouse Clariom S Assay (Thermo Fisher Scientific, Waltham, MA, USA). Genes showing at least a 1.5-fold difference in expression between groups were defined as differentially expressed genes. The gene expression profiles were established using Microarray Data Analysis Tool Ver. 3.2 (Filgen, Nagoya, Japan).

Real-time quantitative PCR

RNA was isolated using an RNeasy mini kit (Qiagen), then complementary DNA was synthesized using SuperScript III (Invitrogen, Waltham, MA, USA) and Random primers (Promega, Madison, WI, USA). Real-time quantitative PCR was carried out in duplicate using a 7500 Fast Real Time PCR system with FAST SYBR Green PCR Master Mix (Applied Biosystems, Foster City, CA, USA). Target mRNA expression was quantified using the comparative cycle threshold method and normalized to that of *Actb*. Table S2 lists the primer sequences used.

Statistical analysis

The results are presented as the mean ± standard deviation. Comparisons between groups were carried out using one-way ANOVA, followed by the Bonferroni test. Statistical significance was accepted at $P < 0.05$.

RESULTS

Effects of glucokinase haploinsufficiency on the glucose tolerance, insulin secretion and β-cell mass of mice consuming an HFHS diet

The bodyweights of the HFHS-fed groups were significantly higher than those of the NC-fed groups after 12 weeks-of-age, irrespective of their genotype (Figure 1a). The fed blood glucose concentrations of the $Gck^{+/-}$NC mice were higher than those of the $Gck^{+/+}$NC mice, because of their genetic background, as previously described[10,30–32]. The $Gck^{+/+}$HFHS mice showed no deterioration in fed blood glucose concentration during the study up to 60 weeks-of-age. $Gck^{+/-}$HFHS mice had high glucose concentrations, but showed no further increase over the long term (Figure 1b). OGTT showed that the glucose tolerance of the $Gck^{+/+}$HFHS mice had not deteriorated by 60 weeks-of-age (Figure 2). The glucose tolerance of the $Gck^{+/-}$HFHS mice did not differ from that of the $Gck^{+/-}$NC mice at 16 weeks-of-age (Figure 2a,d), but had deteriorated by 40 weeks-of-age (Figure 2b,e). Thereafter, however, the area under the glucose curve for the $Gck^{+/-}$HFHS mice at 60 weeks-of-age was not larger than that at 40 weeks, implying that there was no deterioration in glucose tolerance between 40 and 60 weeks-of-age (Figure 2e,f). Insulin resistance, assessed using homeostasis model assessment for insulin resistance was higher in the HFHS-fed than in the NC-fed $Gck^{+/+}$ and $Gck^{+/-}$ mice. However, there was no difference between the $Gck^{+/+}$HFHS mice and the $Gck^{+/-}$HFHS mice (Figure S2).

The GSIS of the $Gck^{+/+}$HFHS mice was higher than that of $Gck^{+/+}$NC mice at 16 weeks-of-age, whereas that of the $Gck^{+/-}$HFHS mice was not larger than that of the $Gck^{+/-}$NC mice (Figure 3a). At 40 weeks-of-age, the GSIS of the $Gck^{+/+}$HFHS mice had further increased, and that of the
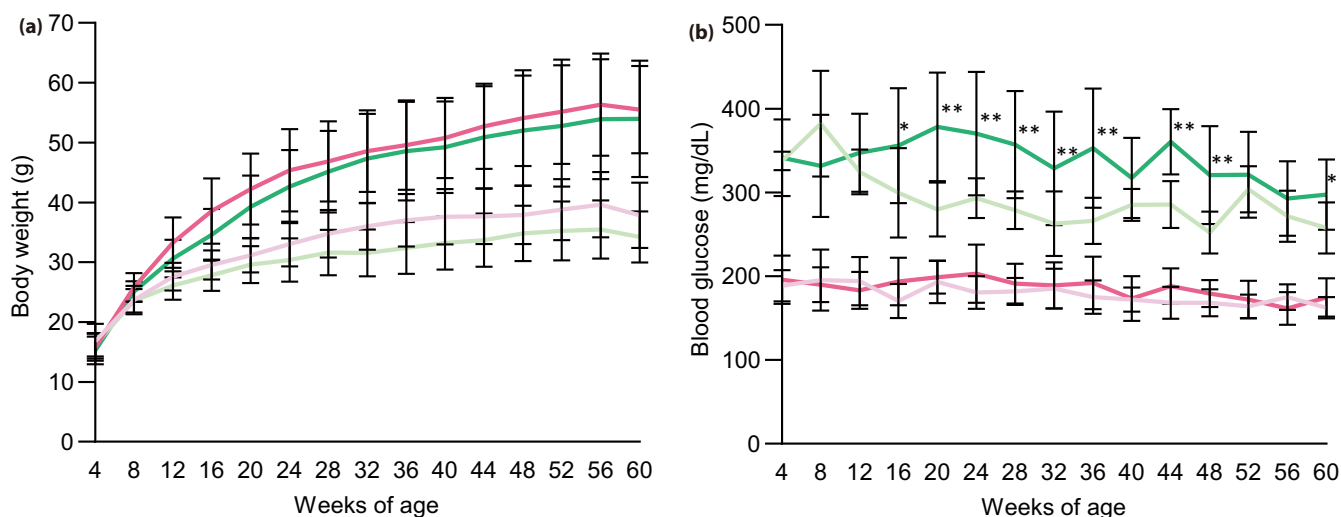

Figure 1 | Bodyweights and blood glucose concentrations of mice in each group up to 60 weeks-of-age. (a) Bodyweights and (b) blood glucose concentrations of $Gck^{+/+}$ normal chow (pale pink line), $Gck^{+/+}$ high-fat, high-sucrose (pink line), $Gck^{+/-}$ normal chow (pale green line) and $Gck^{+/-}$ high-fat, high-sucrose (green line) mice ($n = 11$–20). Data are presented as mean ± standard deviation. **$P < 0.01$, *$P < 0.05$ versus $Gck^{+/-}$ normal chow.
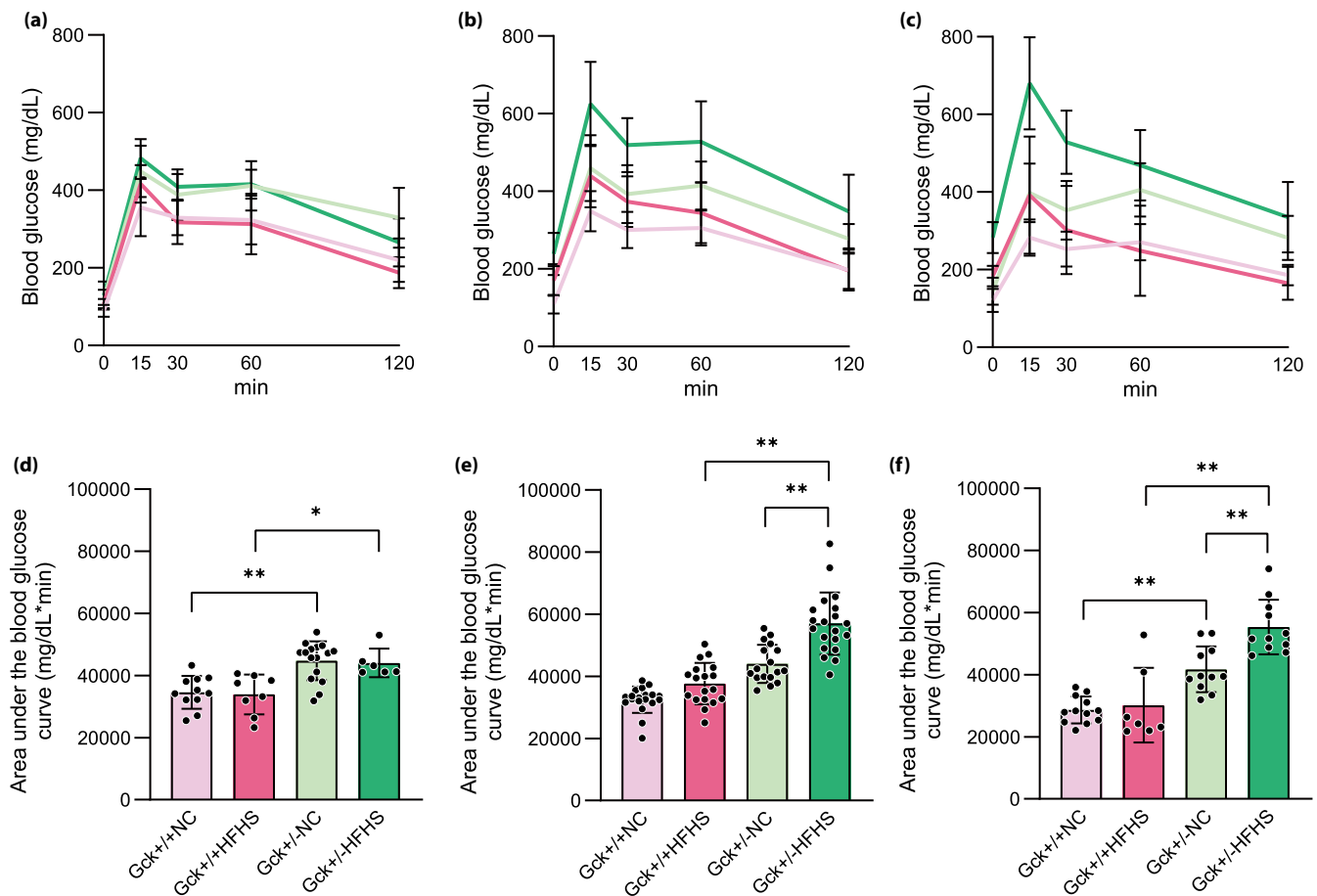
Figure 2 | Glucose tolerance of the mice in each group over time. (a–c) Blood glucose concentrations during oral glucose tolerance testing of the *Gck*^{+/+} normal chow (NC; pale pink line), *Gck*^{+/+} high-fat, high-sucrose (HFHS; pink line), *Gck*^{+/−}NC (pale green line), and *Gck*^{+/−}HFHS (green line) groups at (a) 16 ($n = 6$–16), (b) 40 ($n = 17$–27) and (c) 60 ($n = 7$–12) weeks-of-age. (d–f) Areas under the blood glucose curves during oral glucose tolerance testing of the *Gck*^{+/+}NC (pale pink bar), *Gck*^{+/+}HFHS (pink bar), *Gck*^{+/−}NC (pale green bar) and *Gck*^{+/−}HFHS (green bar) mice at (d) 16, (e) 40 and (f) 60 weeks-of-age. Data are presented as mean ± standard deviation. **$P < 0.01$, *$P < 0.05$.

Gck^{+/−}HFHS mice was higher than that of the *Gck*^{+/−}NC mice (Figure 3b). At 60 weeks-of-age, both the *Gck*^{+/+}HFHS and *Gck*^{+/−}HFHS mice showed further increases in GSIS, and this was more marked in the *Gck*^{+/+}HFHS mice (Figure 3c). Thus, the GSIS of both the *Gck*^{+/+}HFHS and *Gck*^{+/−}HFHS mice increases with time, but the increase in the *Gck*^{+/+}HFHS mice occurs earlier and is more marked.

Figure 4a shows images of pancreatic sections stained for insulin (brown) as a marker of β-cells. There were no significant differences in the β-cell masses of the four groups of mice at 16 weeks-of-age (Figure 4b). At 40 weeks-of-age, the β-cell mass of the *Gck*^{+/+}HFHS mice was larger than that of the *Gck*^{+/+}NC mice, but there was no difference in the masses of the *Gck*^{+/−}HFHS and *Gck*^{+/−}NC mice (Figure 4c). Subsequently, at 60 weeks-of-age, β-cell mass was further increased in *Gck*^{+/+}HFHS mice, and an increasing trend was also observed in *Gck*^{+/−}HFHS mice (Figure 4d). Briefly, β-cell mass was

significantly increased in *Gck*^{+/+}HFHS mice, but also showed an increasing trend in *Gck*^{+/−}HFHS mice.

Effects of glucokinase haploinsufficiency on the islet gene expression of mice consuming an HFHS diet

When we compared the pancreatic islet gene expression profiles of the *Gck*^{+/−}HFHS and *Gck*^{+/+}HFHS mice by DNA microarray analysis, we identified statistically significant, 1.5-fold differences in the expression of 356 of 22,206 genes. Of these, the expression of 128 genes was upregulated and that of 228 genes was downregulated in *Gck*^{+/−}HFHS mice versus *Gck*^{+/+}HFHS mice. The top 20 up- and downregulated genes are listed in Tables 1 and 2. The most downregulated genes included *Spp1*, *Fos*, *Aldh1a3* and *Nupr1*, which have been reported to be upregulated by stress in pancreatic β-cells[33–38]. Pathway analysis was carried out on the up- and downregulated genes, and significant differences were identified in six pathways, including the
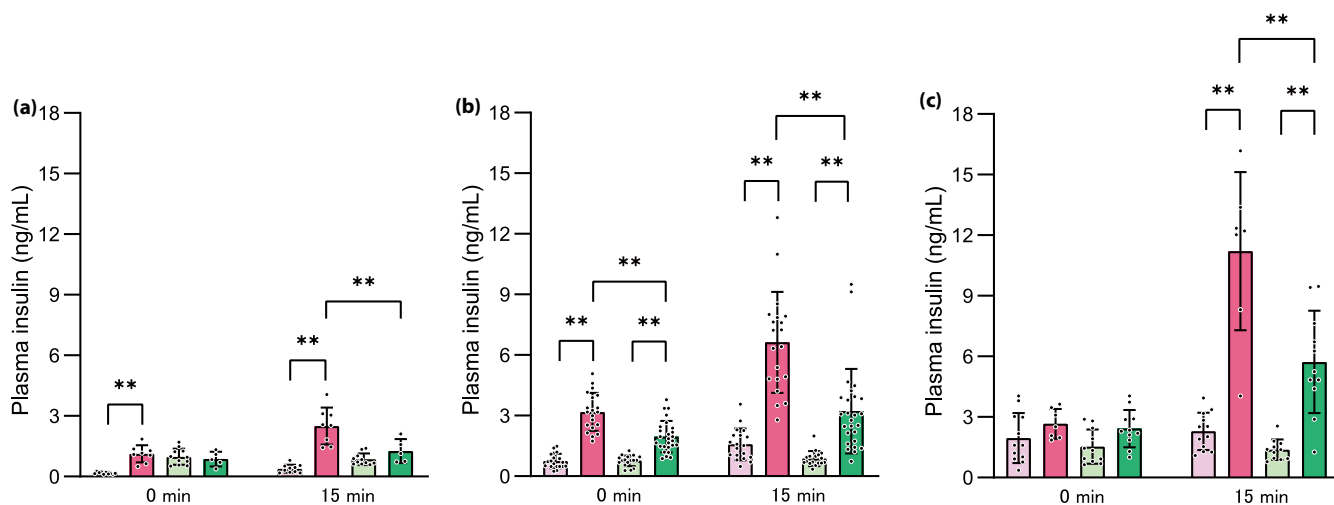
Figure 3 | Glucose-stimulated insulin secretion of the mice in each group over time. Plasma insulin concentrations before and 15 min after glucose loading in the $Gck^{+/+}$ normal chow (pale pink bar), $Gck^{+/+}$ high-fat, high-sucrose (pink bar), $Gck^{+/-}$ normal chow (pale green bar) and $Gck^{+/-}$ high-fat, high-sucrose (green bar) mice at (a) 16 (n = 5–11), (b) 40 (n = 17–26) and (c) 60 (n = 7–12) weeks-of-age. Data are presented as mean ± standard deviation. **P < 0.01.

Jun-Dmp1 and transforming growth factor-β pathways (Table 3).

We next used real-time quantitative PCR analysis to measure the expression of *Ki67*, which is involved in cell proliferation; *Mafa*, *Nkx6.1* and *Pdx1*, which are transcription factors involved in β-cell function; *Slc2a2*, which is responsible for the uptake of glucose by β-cells; and *Spp1*, *Fos*, *Aldh1a3* and *Nupr1*, which were substantially downregulated according to the results of the microarray analysis (Figure 5). Although we showed that $Gck^{+/+}$HFHS mice had high β-cell mass, *Ki67* gene expression, evaluated using real-time quantitative PCR, was higher in $Gck^{+/-}$HFHS mice than in $Gck^{+/-}$NC mice. However, there was no significant difference in the expression of this gene between $Gck^{+/+}$HFHS mice and $Gck^{+/+}$NC mice (Figure 5a). The expression of *Mafa*, *Nkx6.1* and *Pdx1* was not decreased by HFHS diet-feeding in either the $Gck^{+/+}$ or $Gck^{+/-}$ mice (Figure 5b–d). Rather, the expression of *Pdx1* was higher in $Gck^{+/-}$HFHS mice than in $Gck^{+/-}$NC mice, and a similar trend was obtained with respect to the expression of *Mafa* (Figure 5b,d). There were no differences in the expression of *Slc2a2* between the four groups of mice (Figure 5e). Of note, the real-time quantitative PCR analysis showed that *Aldh1a3* was upregulated in $Gck^{+/+}$HFHS mice vs $Gck^{+/+}$NC mice, but not in $Gck^{+/-}$HFHS versus $Gck^{+/-}$NC mice. Its expression was also significantly higher in $Gck^{+/+}$HFHS mice than in $Gck^{+/-}$HFHS mice, consistent with the results of the microarray analysis (Figure 5f). With respect to the other downregulated genes that have previously been reported to be upregulated in pancreatic β-cells in response to stress, the expression of *Nupr1*, but not that of *Spp1* or *Fos*, was significantly lower in $Gck^{+/-}$HFHS mice than in $Gck^{+/+}$HFHS mice (Figure 5g–i).

DISCUSSION

In the present study, HFHS diet-feeding resulted in a deterioration of glucose tolerance in $Gck^{+/-}$ mice because of smaller compensatory increases in β-cell mass and insulin secretion. However, over the long term, there were no further decreases in β-cell mass or insulin secretion, but rather, tendencies for these to increase, and no progressive deterioration of glucose tolerance was identified. Terauchi *et al.*[10] showed that glucokinase is important for the compensatory increase in β-cell mass associated with the feeding of $Gck^{+/+}$ and $Gck^{+/-}$ mice with a high-fat diet for 20 weeks. This finding would suggest that high-fat diet-feeding would lead to a progressive deterioration in the glucose tolerance of $Gck^{+/-}$ mice, and indeed, between 16 and 40 weeks-of-age, the $Gck^{+/-}$HFHS mice in the present study showed a deterioration in glucose tolerance, which was associated with a less substantial increase in β-cell mass than that of $Gck^{+/+}$HFHS mice. Because there was no difference in the insulin resistance of the $Gck^{+/+}$HFHS mice and the $Gck^{+/-}$HFHS mice (Figure S2), we can conclude that glucokinase plays an important role in the compensatory increase in β-cell mass and function that is associated with HFHS diet-feeding, as well as with high-fat diet-feeding. However, over the long term, the $Gck^{+/-}$HFHS mice also showed upward trends in β-cell mass and insulin secretion, suggesting that the pathogenesis of the deterioration in glucose tolerance differs from that of the non-compensatory phase of pancreatic β-cell function, and mass that characterizes in type 2 diabetes (Figure S3).

We fed the same mice used in the high-fat diet-feeding experiment described above a high-starch diet for 15 weeks, and found that glucokinase plays an important role in the compensatory increase in β-cell mass, even when fed this diet[39]. Thus, it has already been shown that the same mechanism

(a)

	16 weeks	40 weeks	60 weeks
Gck+/+NC			
Gck+/+HFHS			
Gck+/-NC			
Gck+/-HFHS			

(b) 16 weeks — β-cell mass (mg): Gck+/+NC, Gck+/+HFHS, Gck+/-NC, Gck+/-HFHS

(c) 40 weeks — β-cell mass (mg): Gck+/+NC, Gck+/+HFHS, Gck+/-NC, Gck+/-HFHS; ** between Gck+/+NC and Gck+/+HFHS; ** between Gck+/+HFHS and Gck+/-HFHS

(d) 60 weeks — β-cell mass (mg): Gck+/+NC, Gck+/+HFHS, Gck+/-NC, Gck+/-HFHS; * between Gck+/+NC and Gck+/-NC; ** between Gck+/+HFHS and Gck+/-HFHS
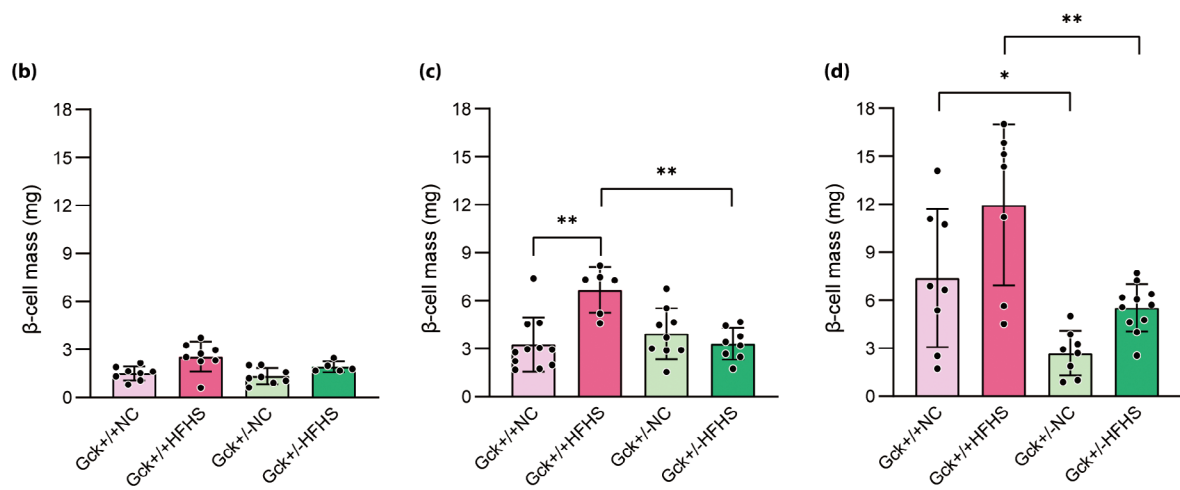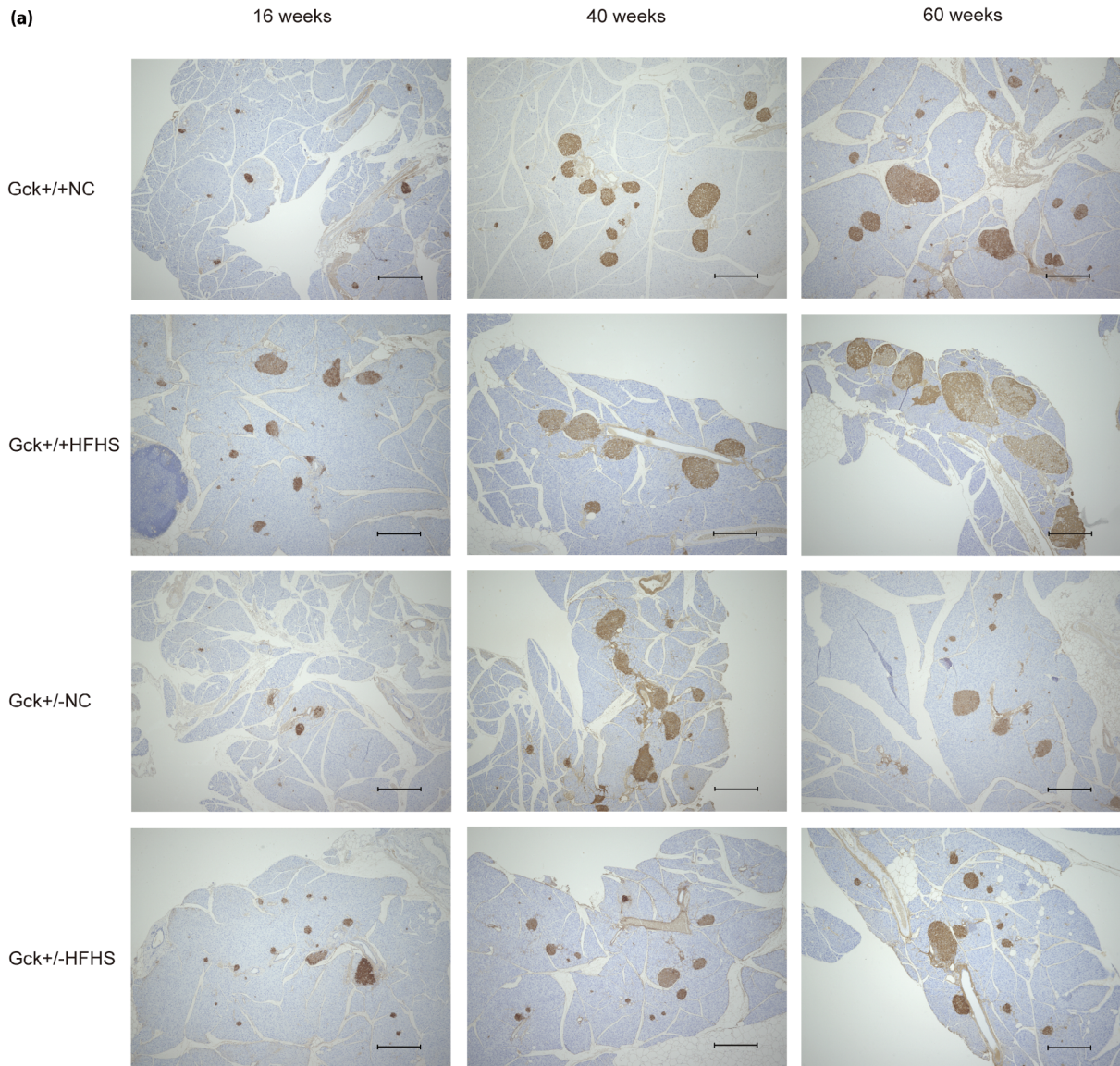
Figure 4 | β-Cell mass of mice in each group over time. (a) Immunohistological analysis of the pancreatic islets of mice in the four groups (Gck$^{+/+}$ normal chow [NC], Gck$^{+/+}$ high-fat, high-sucrose [HFHS], Gck$^{+/-}$NC and Gck$^{+/-}$HFHS mice) at 16, 40 and 60 weeks-of-age. β-Cells are stained brown. Black scale bars represent 500 μm. (b–d) β-Cell masses of the Gck$^{+/+}$NC (pale pink bar), Gck$^{+/+}$HFHS (pink bar), Gck$^{+/-}$NC (pale green bar) and Gck$^{+/-}$HFHS (green bar) groups at (b) 16 (*n* = 5–8), (c) 40 (*n* = 6–11) and (d) 60 (*n* = 7–11) weeks-of-age. Data are presented as mean ± standard deviation. **P < 0.01, *P < 0.05.

Table 1 | Top 20 upregulated genes in the microarray analysis

Gene symbol	Gene accession	*P*-value	Ratio
Nrcam	NM_001146031	0.02950	4.529
Gria3	NM_001281929	0.02421	2.853
Pdk4	NM_013743	0.00748	2.468
Rbp4	NM_001159487	0.02038	2.303
Slc16a7	NM_011391	0.04280	2.233
Hrh3	NM_133849	0.00395	2.204
Rab3c	NM_023852	0.02065	2.198
1700086L19Rik	NR_030733	0.04217	2.191
Pcdh15	NM_001142735	0.03069	2.181
Myo3a	NM_148413	0.00016	2.175
Dpp10	NM_199021	0.04415	2.154
Fbxo47	NM_001081435	0.03417	2.098
Galnt13	NM_173030	0.02984	2.078
Scn3b	NM_001083917	0.04781	2.075
Ptprz1	NM_001081306	0.03182	2.049
Asic2	NM_001034013	0.01799	2.027
Epb41l4a	NM_013512	0.00189	2.023
Hcar1	NM_175520	0.02590	2.022
Ankrd34c	NM_207260	0.00601	2.006
Dpp6	NM_001136060	0.03635	2.003

Table 2 | Top 20 downregulated genes in the microarray analysis

Gene symbol	Gene accession	*P*-value	Ratio
Spp1	NM_001204201	0.00355	0.071
Gucy2c	NM_001127318	0.01929	0.208
Fos	NM_010234	0.00940	0.283
Necab2	NM_054095	0.00305	0.290
Dapl1	NM_029723	0.00745	0.306
Rasd2	NM_029182	0.00259	0.312
Gm3298	ENSMUST00000165289	0.02709	0.342
Aldh1a3	NM_053080	0.01939	0.350
Fabp4	NM_024406	0.01750	0.360
Serpina7	NM_177920	0.00559	0.365
Nupr1	NM_019738	0.02311	0.374
Cpne4	NM_028719	0.00799	0.374
Creld2	NM_029720	0.04892	0.378
Rasl10b	NM_001013386	0.01203	0.387
Jchain	NM_152839	0.03197	0.393
Apof	NM_133997	0.00135	0.397
Gm8281	ENSMUST00000100893	0.03760	0.405
Gabra4	NM_010251	0.00058	0.411
Pcp4	NM_008791	0.04728	0.413
Thbs1	NM_011580	0.01510	0.419

Table 3 | Results of the pathway analysis carried out using the microarray data

Pathway	Total	Up	Down	*P*-value	Up list	Down list
Mm_Triacylglyceride_synthesis_WP386_117951	23	2	1	0.009607	Lpl, Gk	Plpp1
Mm_Novel_Jun-Dmp1_pathway_WP3654_116721	26	0	3	0.013013		Jun, Fos, Myc
Mm_TGF-beta_signaling_pathway_WP113_116497	52	0	4	0.015194		Thbs1, Jun, Spp1, Fos
Mm_Electron_transport_chain_WP295_117879	94	0	5	0.027087		Cox6a1, Ndufs7, Atp5o, Ndufs8, Cox8a
Mm_Retinol_metabolism_WP1259_106842	39	2	1	0.034876	Lpl, Rbp4	Aldh1a3
Mm_GPCRs,_peptide_WP234_117936	69	3	1	0.036202	Avpr1b, Cxcr6, Sstr2	Ednrb

underpins the compensatory increases in β-cell mass that occur in response to high-fat and high-starch diet-feeding. What makes the present study different from the previous two studies is the composition of the diet and the long study period. The reason we used an HFHS diet was to increase the level of stress placed on the β-cells. The HFHS diet used in the present study contains a high proportion of saturated fatty acids. Palmitic acid, a saturated fatty acid, has been reported to induce the dysfunction of β-cells[40]. However, the present study was carried out under ad libitum feeding conditions, and the increases in bodyweight and blood glucose concentration seemed to be smaller than those achieved by high-fat diet-feeding (data not

shown). Therefore, it is not known whether the HFHS diet-feeding increased the stress on the β cells. However, the length of the study period is a strength of the present study. Through longer-term observations, it has become clear that glucokinase haploinsufficiency slows the development of the phenotype, but does not result in a loss of the potential for an increase in β-cell mass over the long term.

Another important finding of the present study is that the *Aldh1a3* expression in pancreatic islets was high in Gck$^{+/+}$HFHS mice, but not in Gck$^{+/-}$HFHS mice. Aldehyde dehydrogenase activities typically increase in response to stress, and, therefore, the metabolism of endogenous and exogenous
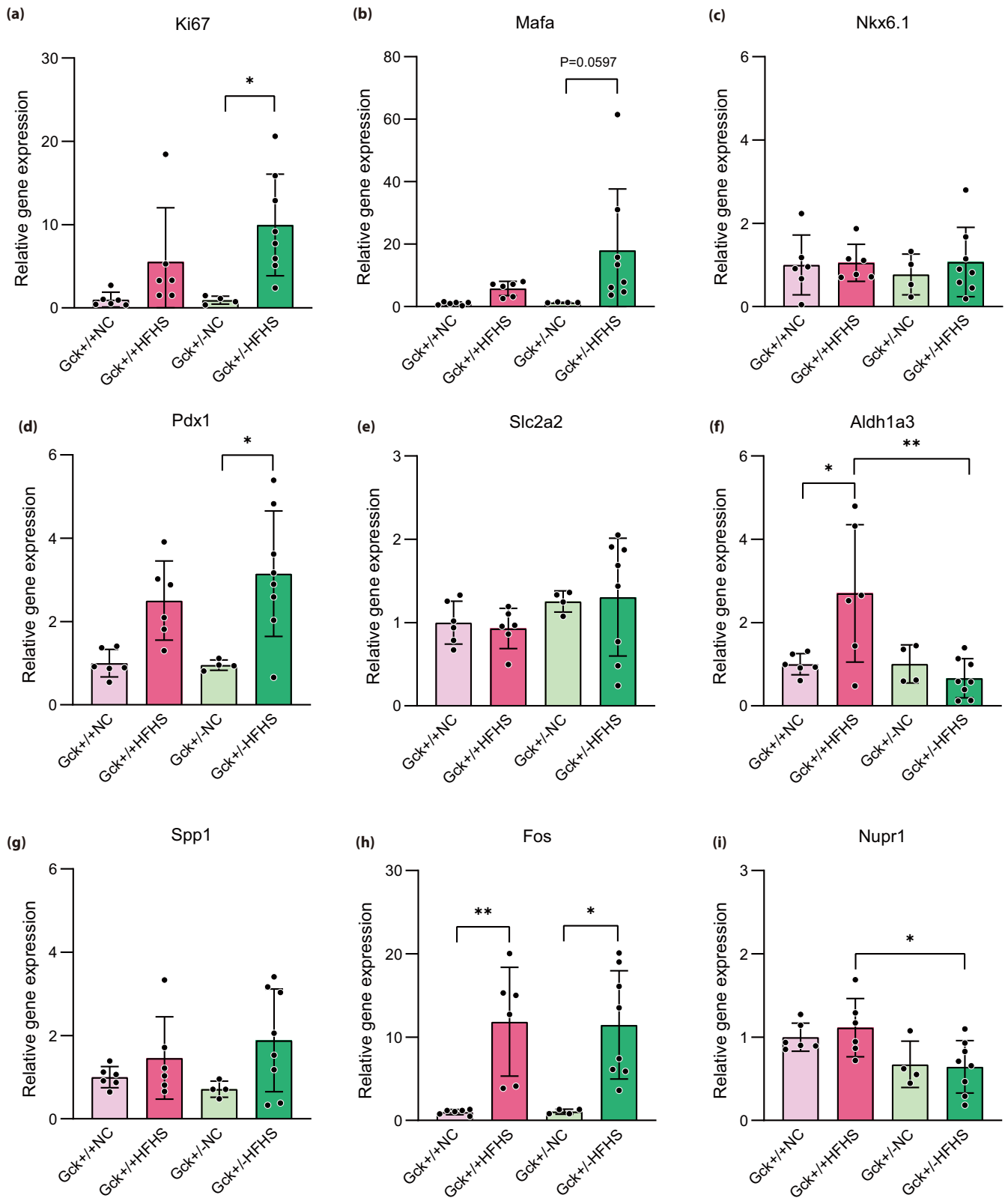
Figure 5 | Expression of key genes in the pancreatic islets of mice in each group at 40 weeks-of-age. Expression of the *Ki67, Mafa, Nkx6.1, Pdx1, Slc2a2, Aldh1a3, Spp1, Fos* and *Nupr1* genes in the *Gck*+/+ normal chow (NC; pale pink bar), *Gck*+/+ high-fat, high-sucrose [HFHS; pink bar], *Gck*+/−NC (pale green bar) and *Gck*+/−HFHS (green bar) groups at 40 weeks-of-age (*n* = 4–8). Data are normalized to the expression of *Actb* and are presented as mean ± standard deviation. **P < 0.01, *P < 0.05.

aldehydes increases, thereby reducing oxidative stress and lipid peroxidation[35]. Although no previous studies have identified the mechanism by which *Aldh1a3* expression is upregulated in pancreatic islets, Shimamura *et al.*[36] showed that *Aldh1a3* expression in pancreatic islets is high in mice with high-fat diet-induced diabetes and *db/db* mice with poor glucose tolerance. Another study showed that *Aldh1a3* expression is high in various models of diabetes, and that high *Aldh1a3* expression is a common feature of diabetic β-cells[41]. Indeed, Son *et al.*[42] showed that *db/db* mice with β-cell-specific knockout of *Aldh1a3* show superior glucose tolerance and insulin secretion. These data imply that *Aldh1a3* expression is associated with pancreatic β-cell function.

In the present study, although the β-cell mass and insulin secretion of the $Gck^{+/+}$HFHS mice were substantially higher than those of mice fed normal chow, the high expression of *Aldh1a3* suggests that a higher level of metabolic stress and poorer pancreatic β-cell function were also present. In contrast, $Gck^{+/-}$HFHS mice did not show high *Aldh1a3*, suggesting that even when their β-cells are challenged by a high glucose load, they have a low level of metabolic stress, owing to less post-glucokinase metabolic signaling, which prevents the deterioration of pancreatic β-cell mass and function. The associated upregulation of the Jun-Dmp1 and transforming growth factor-β pathways identified using pathway analysis of the DNA microarray analysis data (the appropriate genes were downregulated in $Gck^{+/-}$HFHS mice vs $Gck^{+/+}$HFHS mice), and the low *Nupr1* expression identified using DNA microarray analysis and real-time quantitative PCR analysis are consistent with this contention. *Aldh1a3* expression is also known to be upregulated in association with β-cell dedifferentiation[43]. The higher *Aldh1a3* mRNA expression in the $Gck^{+/+}$HFHS mice versus the $Gck^{+/-}$HFHS mice might indicate that the HFHS diet induces such dedifferentiation in the $Gck^{+/+}$ mice. However, there was no difference in the expression of *Neurog3*, a marker of islet progenitor cells, between the $Gck^{+/+}$HFHS mice and the $Gck^{+/-}$HFHS mice, as shown by DNA microarray analysis (ratio 1.209, $P = 0.40$) and real-time quantitative PCR (Figure S4). Therefore, to determine whether dedifferentiation is part of the phenotype, further research is needed.

As mentioned in the Introduction, we previously established and analyzed $Gck^{+/-}db/db$ mice, and reported that glucokinase haploinsufficiency improves intracellular metabolism, and preserves pancreatic β-cell mass and function in *db/db* mice[29,30]. The results of the present study of HFHS-fed mice suggest that glucokinase haploinsufficiency also prevents the progressive decline in pancreatic β-cell mass and function in this model. However, we identified some differences between the findings obtained using this model and those of our previous study of *db/db* mice. We found that $Gck^{+/+}db/db$ mice experience a marked deterioration in glucose tolerance, but the glucose tolerance of $Gck^{+/+}$HFHS mice was found not to deteriorate up to 60 weeks-of-age. Furthermore, the *db/db*

mice showed significantly lower expression of the *Ki67*, *Mafa*, *Nkx6.1* and *Pdx1* genes in the pancreatic islets of $Gck^{+/+}db/db$ mice than in those of $Gck^{+/-}db/db$ mice, although there were no significant differences between $Gck^{+/+}$HFHS and $Gck^{+/-}$HFHS mice in the present study. This might be because the glucose load on the β-cells induced by long-term HFHS diet-feeding was much lower than that of *db/db* mice. Therefore, another model of diet-induced obesity and diabetes in which glucose tolerance is impaired should be established for future studies. This model would more clearly show the protective effect of glucokinase inhibition on pancreatic β-cells.

In conclusion, glucokinase haploinsufficiency prevents the progressive deterioration of pancreatic β-cell mass/function and glucose tolerance in long-term HFHS diet-fed mice.

DISCLOSURE

The authors declare no conflict of interest.
Approval of the research protocol: N/A.
Informed Consent: N/A.
Approval date of Registry and the Registration No. of the study/trial: N/A.
Animal Studies: The study was approved by the Animal Use Committee of Hokkaido University Graduate School of Medicine, and was carried out in accordance with the Animal Use Guidelines of Hokkaido University (approval numbers: 18-0033 [until 3/31/2023] and 23-0078 [from 4/1/2023]).

REFERENCES

1. Collaborators GBDD. Global, regional, and national burden of diabetes from 1990 to 2021, with projections of prevalence to 2050: A systematic analysis for the Global Burden of Disease Study 2021. *Lancet* 2023; 402: 203–234.
2. Weir GC, Gaglia J, Bonner-Weir S. Inadequate beta-cell mass is essential for the pathogenesis of type 2 diabetes. *Lancet Diabetes Endocrinol* 2020; 8: 249–256.
3. Eizirik DL, Pasquali L, Cnop M. Pancreatic beta-cells in type 1 and type 2 diabetes mellitus: Different pathways to failure. *Nat Rev Endocrinol* 2020; 16: 349–362.

4. Yagihashi S, Inaba W, Mizukami H. Dynamic pathology of islet endocrine cells in type 2 diabetes: Beta-cell growth, death, regeneration and their clinical implications. *J Diabetes Investig* 2016; 7: 155–165.

5. Kendall DM, Cuddihy RM, Bergenstal RM. Clinical application of incretin-based therapy: Therapeutic potential, patient selection and clinical use. *Am J Med* 2009; 122: S37–S50.

6. Butler AE, Janson J, Bonner-Weir S, *et al*. Beta-cell deficit and increased beta-cell apoptosis in humans with type 2 diabetes. *Diabetes* 2003; 52: 102–110.

7. Kassem S, Bhandari S, Rodriguez-Bada P, *et al*. Large islets, beta-cell proliferation, and a glucokinase mutation. *N Engl J Med* 2010; 362: 1348–1350.

8. Nakamura A. Glucokinase as a therapeutic target based on findings from the analysis of mouse models. *Endocr J* 2022; 69: 479–485.

9. Porat S, Weinberg-Corem N, Tornovsky-Babaey S, *et al*. Control of pancreatic beta cell regeneration by glucose metabolism. *Cell Metab* 2011; 13: 440–449.

10. Terauchi Y, Takamoto I, Kubota N, *et al*. Glucokinase and IRS-2 are required for compensatory beta cell hyperplasia in response to high-fat diet-induced insulin resistance. *J Clin Invest* 2007; 117: 246–257.

11. Matschinsky FM, Wilson DF. The central role of glucokinase in glucose homeostasis: A perspective 50 years after demonstrating the presence of the enzyme in islets of Langerhans. *Front Physiol* 2019; 10: 148.

12. Matschinsky FM, Magnuson MA, Zelent D, *et al*. The network of glucokinase-expressing cells in glucose homeostasis and the potential of glucokinase activators for diabetes therapy. *Diabetes* 2006; 55: 1–12.

13. Zhu D, Li X, Ma J, *et al*. Dorzagliatin in drug-naive patients with type 2 diabetes: A randomized, double-blind, placebo-controlled phase 3 trial. *Nat Med* 2022; 28: 965–973.

14. Yang W, Zhu D, Gan S, *et al*. Dorzagliatin add-on therapy to metformin in patients with type 2 diabetes: A randomized, double-blind, placebo-controlled phase 3 trial. *Nat Med* 2022; 28: 974–981.

15. Toulis KA, Nirantharakumar K, Pourzitaki C, *et al*. Glucokinase activators for type 2 diabetes: Challenges and future developments. *Drugs* 2020; 80: 467–475.

16. Vella A, Freeman JLR, Dunn I, *et al*. Targeting hepatic glucokinase to treat diabetes with TTP399, a hepatoselective glucokinase activator. *Sci Transl Med* 2019; 11: eaau3441.

17. Zhu D, Gan S, Liu Y, *et al*. Dorzagliatin monotherapy in Chinese patients with type 2 diabetes: A dose-ranging, randomised, double-blind, placebo-controlled, phase 2 study. *Lancet Diabetes Endocrinol* 2018; 6: 627–636.

18. Grimsby J, Sarabu R, Corbett WL, *et al*. Allosteric activators of glucokinase: Potential role in diabetes therapy. *Science* 2003; 301: 370–373.

19. Zhu XX, Zhu DL, Li XY, *et al*. Dorzagliatin (HMS5552), a novel dual-acting glucokinase activator, improves glycaemic

control and pancreatic beta-cell function in patients with type 2 diabetes: A 28-day treatment study using biomarker-guided patient selection. *Diabetes Obes Metab* 2018; 20: 2113–2120.

20. Nakamura A, Togashi Y, Orime K, *et al*. Control of beta cell function and proliferation in mice stimulated by small-molecule glucokinase activator under various conditions. *Diabetologia* 2012; 55: 1745–1754.

21. Nakamura A, Terauchi Y, Ohyama S, *et al*. Impact of small-molecule glucokinase activator on glucose metabolism and beta-cell mass. *Endocrinology* 2009; 150: 1147–1154.

22. Kawata S, Nakamura A, Miyoshi H, *et al*. Glucokinase activation leads to an unsustained hypoglycaemic effect with hepatic triglyceride accumulation in db/db mice. *Diabetes Obes Metab* 2022; 24: 391–401.

23. Nakamura A, Terauchi Y. Present status of clinical deployment of glucokinase activators. *J Diabetes Investig* 2015; 6: 124–132.

24. Wilding JP, Leonsson-Zachrisson M, Wessman C, *et al*. Dose-ranging study with the glucokinase activator AZD1656 in patients with type 2 diabetes mellitus on metformin. *Diabetes Obes Metab* 2013; 15: 750–759.

25. Kiyosue A, Hayashi N, Komori H, *et al*. Dose-ranging study with the glucokinase activator AZD1656 as monotherapy in Japanese patients with type 2 diabetes mellitus. *Diabetes Obes Metab* 2013; 15: 923–930.

26. Meininger GE, Scott R, Alba M, *et al*. Effects of MK-0941, a novel glucokinase activator, on glycemic control in insulin-treated patients with type 2 diabetes. *Diabetes Care* 2011; 34: 2560–2566.

27. Tornovsky-Babeay S, Weinberg-Corem N, Ben-Haroush Schyr R, *et al*. Biphasic dynamics of beta cell mass in a mouse model of congenital hyperinsulinism: Implications for type 2 diabetes. *Diabetologia* 2021; 64: 1133–1143.

28. Tornovsky-Babeay S, Dadon D, Ziv O, *et al*. Type 2 diabetes and congenital hyperinsulinism cause DNA double-strand breaks and p53 activity in beta cells. *Cell Metab* 2014; 19: 109–121.

29. Nakamura A, Omori K, Terauchi Y. Glucokinase activation or inactivation: Which will lead to the treatment of type 2 diabetes? *Diabetes Obes Metab* 2021; 23: 2199–2206.

30. Omori K, Nakamura A, Miyoshi H, *et al*. Glucokinase inactivation paradoxically ameliorates glucose intolerance by increasing beta-cell mass in db/db mice. *Diabetes* 2021; 70: 917–931.

31. Terauchi Y, Sakura H, Yasuda K, *et al*. Pancreatic β-cell-specific targeted disruption of glucokinase gene. *J Biol Chem* 1995; 270: 30253–30256.

32. Terauchi Y, Iwamoto K, Tamemoto H, *et al*. Development of non-insulin-dependent diabetes mellitus in the double knockout mice with disruption of insulin receptor substrate-1 and beta cell glucokinase genes. Genetic reconstitution of diabetes as a polygenic disease. *J Clin Invest* 1997; 99: 861–866.

33. Icer MA, Gezmen-Karadag M. The multiple functions and mechanisms of osteopontin. *Clin Biochem* 2018; 59: 17–24.

34. Priya Dharshini LC, Vishnupriya S, Sakthivel KM, *et al*. Oxidative stress responsive transcription factors in cellular signalling transduction mechanisms. *Cell Signal* 2020; 72: 109670.

35. Singh S, Brocker C, Koppaka V, *et al*. Aldehyde dehydrogenases in cellular responses to oxidative/electrophilic stress. *Free Radic Biol Med* 2013; 56: 89–101.

36. Shimamura M, Karasawa H, Sakakibara S, *et al*. Raldh3 expression in diabetic islets reciprocally regulates secretion of insulin and glucagon from pancreatic islets. *Biochem Biophys Res Commun* 2010; 401: 79–84.

37. Path G, Mehana AE, Pilz IH, *et al*. NUPR1 preserves insulin secretion of pancreatic beta-cells during inflammatory stress by multiple low-dose streptozotocin and high-fat diet. *Am J Physiol Endocrinol Metab* 2020; 319: E338–E344.

38. Mallo GV, Fiedler F, Calvo EL, *et al*. Cloning and expression of the rat p8 cDNA, a new gene activated in pancreas during the acute phase of pancreatitis, pancreatic development, and regeneration, and which promotes cellular growth. *J Biol Chem* 1997; 272: 32360–32369.

39. Tsuchida K, Nakamura A, Miyoshi H, *et al*. Glucokinase is required for high-starch diet-induced beta-cell mass expansion in mice. *J Diabetes Investig* 2021; 12: 1545–1554.

40. Eguchi K, Manabe I, Oishi-Tanaka Y, *et al*. Saturated fatty acid and TLR signaling link beta cell dysfunction and islet inflammation. *Cell Metab* 2012; 15: 518–533.

41. Kim-Muller JY, Fan J, Kim YJ, *et al*. Aldehyde dehydrogenase 1a3 defines a subset of failing pancreatic beta cells in diabetic mice. *Nat Commun* 2016; 7: 12631.

42. Son J, Du W, Esposito M, *et al*. Genetic and pharmacologic inhibition of ALDH1A3 as a treatment of beta-cell failure. *Nat Commun* 2023; 14: 558.

43. Cinti F, Bouchi R, Kim-Muller JY, *et al*. Evidence of beta-cell dedifferentiation in human type 2 diabetes. *J Clin Endocrinol Metab* 2016; 101: 1044–1054.

SUPPORTING INFORMATION

Additional supporting information may be found online in the Supporting Information section at the end of the article.

Figure S1. Expression of *Gck* in the pancreatic islets of mice in NC-fed groups.

Figure S2. HOMA-IR of the mice in each group at 40 weeks of age.

Figure S3. Changes of β-cell mass and function over time in HFHS-fed groups.

Figure S4. Expression of *Neurog3* in the pancreatic islets of mice in the HFHS-fed groups at 40 weeks of age.

Table S1. Energy composition of the diets.

Table S2. Sequences of the primers used for real-time quantitative PCR.